Fermi level effects on Mn incorporation in modulation-doped ferromagnetic $III_{1-x}Mn_xV$ heterostructures

2004 J. Phys.: Condens. Matter 16 S5499

(http://iopscience.iop.org/0953-8984/16/48/004)

INSTITUTE OF PHYSICS PUBLISHING JOURNAL OF PHYSICS: CONDENSED MATTER

J. Phys.: Condens. Matter **16** (2004) S5499–S5508 PII: S0953-8984(04)79188-2

Fermi level effects on Mn incorporation in modulation-doped ferromagnetic $III_{1-x}Mn_xV$ heterostructures

J K Furdyna[1], T Wojtowicz[1,2], X Liu[1], K M Yu[3], W Walukiewicz[3], I Vurgaftman[4] and J R Meyer[4]

[1] Department of Physics, University of Notre Dame, Notre Dame, IN 46556, USA
[2] Institute of Physics, Polish Academy of Sciences, 02-668 Warsaw, Poland
[3] Materials Sciences Division, Lawrence Berkeley National Laboratory, Berkeley, CA 94720, USA
[4] Code 5613, Naval Research Laboratory, Washington, DC 20375, USA

Received 13 April 2004
Published 19 November 2004
Online at stacks.iop.org/JPhysCM/16/S5499
doi:10.1088/0953-8984/16/48/004

Abstract

The effect of increasing the Fermi level by modulation doping on the incorporation of Mn into the III–V host lattice—and hence on the ferromagnetic properties of $III_{1-x}Mn_xV$ alloys—is investigated in $Ga_{1-x}Mn_xAs/Ga_{1-y}Al_yAs$ heterojunctions and quantum wells. Introducing Be acceptors into the $Ga_{1-y}Al_yAs$ barriers leads to an increase of the Curie temperature T_C of $Ga_{1-x}Mn_xAs$, from 70 K in undoped structures to over 100 K in modulation-doped structures. This increase is qualitatively consistent with multi-band mean field theory simulation of carrier-mediated ferromagnetism. Here the crucial feature is that the increase of T_C occurs only in those structures where the modulation doping is introduced *after* the deposition of the magnetic layer, and that T_C actually drops when the Be-doped layer is grown first. Using ion channelling techniques we provide direct evidence that this latter reduction in T_C is directly correlated with an increased formation of magnetically inactive Mn interstitials. This formation of interstitials is induced by the shift of the Fermi energy as the holes are transferred from the barrier to the quantum well during the growth.

1. Introduction

Substitutional incorporation of Mn into the III–V lattice in sufficient concentrations to form ferromagnetic $III_{1-x}Mn_xV$ alloys (e.g., $Ga_{1-x}Mn_xAs$) must be carried out by non-equilibrium low-temperature epitaxy, whereby Mn concentrations of a few per cent can be obtained [1]. The ferromagnetism of these alloys occurs because, in addition to providing magnetic moments, the Mn ions also act as acceptors, thus supplying large concentrations of holes that mediate the

ferromagnetic interaction between magnetic moments of the Mn ions [2]. The mean field theory predicts that the Curie temperature T_C should scale as the product of the Mn concentration x and of the hole density p. Thus in principle above-room-temperature ferromagnetism could occur in these materials for sufficiently large values of the product xp [3].

Our research on $Ga_{1-x}Mn_xAs$ and $In_{1-x}Mn_xSb$ semiconductor layers has shown, however, that the Fermi energies achievable in these materials cannot exceed a certain maximum E_{Fmax}, which puts a limit on the maximum value of the hole concentrations p_{max}. This occurs because the relationship between the formation energies for negatively-charged defects (such as the desired substitutional Mn acceptors Mn_{III}, e.g., Mn_{Ga} or Mn_{In}) and positively-charged defects (such as the unwanted interstitial Mn double donors, Mn_I) is controlled by the Fermi energy. When E_F in the $III_{1-x}Mn_xV$ reaches E_{Fmax} due to the increasing free hole density, further formation of Mn_{III} becomes energetically too costly, and compensating Mn_I defects begin to form. This occurs whenever the hole concentration p approaches p_{max} either due to a high concentration of Mn acceptors, e.g., in $Ga_{1-x}Mn_xAs$ [4] and $In_{1-x}Mn_xSb$ [5, 6]; or due to the combined number of Mn and of nonmagnetic Be acceptors, as in $Ga_{1-x-y}Mn_xBe_yAs$ [5, 7, 8] and $In_{1-x-y}Mn_xBe_ySb$ [9]. Additionally, an increasing number of Mn begins to collect in the form of random clusters (incommensurate with the III–V lattice), that donate neither holes nor spins to the system.

The creation of Mn_I is deleterious to the ferromagnetism for multiple reasons. First, compensation by the double Mn_I donors reduces the hole concentration; second, it has been shown theoretically that interstitial Mn is RKKY-inactive due to its negligible p–d exchange [10]; and, finally, Mn_I forms antiferromagnetic pairs with Mn_{III} [4, 10], further reducing the density of Mn ions that contribute to the ferromagnetism of the $III_{1-x}Mn_xV$ alloy. Thus any increase of the Mn_I concentration automatically leads to a lowering of the value of T_C.

Our ion-channelling experiments directly revealed this type of interstitial Mn creation whenever p approaches p_{max} due to either a high Mn concentration [4] or a high combined concentration of Mn and Be [8]. In this paper we concentrate on showing that substitutional versus interstitial incorporation of Mn in $III_{1-x}Mn_xV$ alloys is determined by the Fermi energy *during the growth process itself*, no matter what is the source of the holes that establish the value of E_F, and independent of the spatial location of the acceptors with respect to the magnetic Mn ions. To demonstrate this, we use growth experiments involving modulation doping of $Ga_{1-x}Mn_xAs/Ga_{1-y}Al_yAs$ heterostructures by Be—an approach that allows us to vary the Fermi level in the $Ga_{1-x}Mn_xAs$ layer *independently* of the Mn concentration within that layer.

2. Experimental procedures

Ferromagnetic $III_{1-x}Mn_xV$ heterostructures used in our research were grown by molecular beam epitaxy in a Riber 32 R&D MBE system. Fluxes of Ga, Be, and Mn were supplied by standard effusion cells, while the As_2 flux was produced by cracker cells. (001)-oriented GaAs wafers with high-temperature-grown GaAs buffers were used as substrates. The substrate temperature for the growth of all heterostructures was kept constant at the same low temperature of 210 °C. Three distinct series of samples were grown. The first two series were heterojunctions, consisting of 5.6 nm $Ga_{1-x}Mn_xAs$ layers followed by 13.5 nm $Ga_{0.76}Al_{0.24}As$ barriers. The barriers were modulation-doped (MD) with Be at a distance of 1 monolayer away from $Ga_{1-x}Mn_xAs$. In the first series (with $x = 0.062$), the temperature of the Be source T_{Be} was kept constant at 1040 °C, and three different doping-layer thicknesses were employed ($d_{Be} = 0$, 5.3, and 13.2 nm). In the second series ($x = 0.066$), d_{Be} was kept constant at 13.2 nm, and the Be concentration was varied by changing T_{Be} ($T_{Be} = 0$, 1020, 1040 and 1050 °C). Finally, in addition to the above heterojunctions, we

also grew three $Ga_{0.76}Al_{0.24}As/Ga_{1-x}Mn_xAs/Ga_{0.76}Al_{0.24}As$ quantum well (QW) structures, with Be doping in one of the two barriers (introduced either *before* or *after* growing the $Ga_{1-x}Mn_xAs$ QW). The width of the QW was 5.6 nm, with Mn concentration $x = 0.062$, the total thickness of each barrier was 13.5 nm, and d_{Be} was 13.2 nm in all the latter structures.

Resistivity, Hall effect, and SQUID measurements were used for electrical and magnetic characterization of the samples, and for determining T_C. The total Mn concentration x and the location of the Mn atoms in the III–V lattice were established by simultaneous channelling Rutherford backscattering spectrometry (c-RBS) and channelling particle induced x-ray emission (c-PIXE) measurements using a 1.95 MeV $^4He^{2+}$ beam [4, 8]. Back-scattered He ions and characteristic x-rays excited by the He ions were detected by an Si surface barrier detector located at a backscattering angle of 165°, and an Si(Li) detector located at 30° with respect to the incident ion beam, respectively. The specific locations of Mn atoms in the $Ga_{1-x}Mn_xAs$ lattice were determined by directly comparing the angular scans about the ⟨110⟩ and ⟨111⟩ axial channels of the Mn Kα x-ray signals (PIXE) with those of the RBS signals from the III–V host lattice. The normalized yield χ for the RBS (χ_{GaAs}) and for the PIXE Mn x-ray signals (χ_{Mn}), discussed later in this paper, are defined as the ratio of the channelled yield to the corresponding unaligned yield.

3. Experimental results and discussion

Based on our previous experimental studies of $III_{1-x}Mn_xV$ layers, one would expect a strong increase of the Mn_I concentration at the expense of Mn_{III} whenever E_F increases due to the transfer of holes from a modulation-doped barrier into the $III_{1-x}Mn_xV$ alloy QW. However, increasing the value of E_F affects the creation of Mn_I only when the additional holes *are already present* during the $III_{1-x}Mn_xV$ growth, i.e., when the Be-doped layer is grown *before depositing* $III_{1-x}Mn_xV$. Thus in the case of $Ga_{1-y}Al_yAs/Ga_{1-x}Mn_xAs/Ga_{1-y}Al_yAs$ structures—where $Ga_{1-x}Mn_xAs$ acts as a quantum well (QW)—one expects an increase of T_C when the doped barrier is grown *after* the $Ga_{1-x}Mn_xAs$ deposition (because then the value of p increases after the ferromagnetically-active region has already been formed), but a drop of T_C when the Be-doped barrier is deposited *before* the QW (because then the larger value of E_F during the growth due to the holes arriving from the barrier prevents incorporation of Mn_{III}, inducing instead the creation of Mn_I).

We begin by discussing experimental result demonstrating that the Curie temperature of the $III_{1-x}Mn_xV$ ferromagnetic semiconductor can be increased by modulation doping in low-temperature-grown structures when the acceptors are introduced *after* the magnetic layer has already been grown. The temperature dependence of zero-field resistivities ρ for MD heterojunctions in which Be-doped $Ga_{1-y}Al_yAs$ was grown *after* depositing $Ga_{1-x}Mn_xAs$ is presented in figure 1. All of the samples show a clear resistivity peak at a temperature T_ρ, which may be taken as a convenient marker of T_C [11]. The data for samples in which the thickness of the Be-doped region d_{Be} was varied while keeping the Be flux constant are shown in the left-hand panel. One can see that T_ρ increases from 77 K in the undoped structure ($d_{Be} = 0$) to ≈98 K for $d_{Be} = 5.3$ nm, and to 110 K for $d_{Be} = 13.2$ nm. To further test the enhancement of T_C with increasing Be concentration in the barrier, we studied a series of specimens with a constant d_{Be} but grown with various T_{Be}. The results for this series are shown in the right-hand panel of figure 1. Additionally, data for a 67 nm-thick $Ga_{1-x}Mn_xAs$ epilayer with the same Mn concentration ($x = 0.066$) are also shown as the open symbols. While all of the undoped samples grown under the same conditions (three heterostructures and one layer) have very similar values of T_ρ (72–75 K), the doped structures all have higher T_ρ, ranging from 95 K (for $T_{Be} = 1020\,°C$) to 110 K ($T_{Be} = 1050\,°C$).

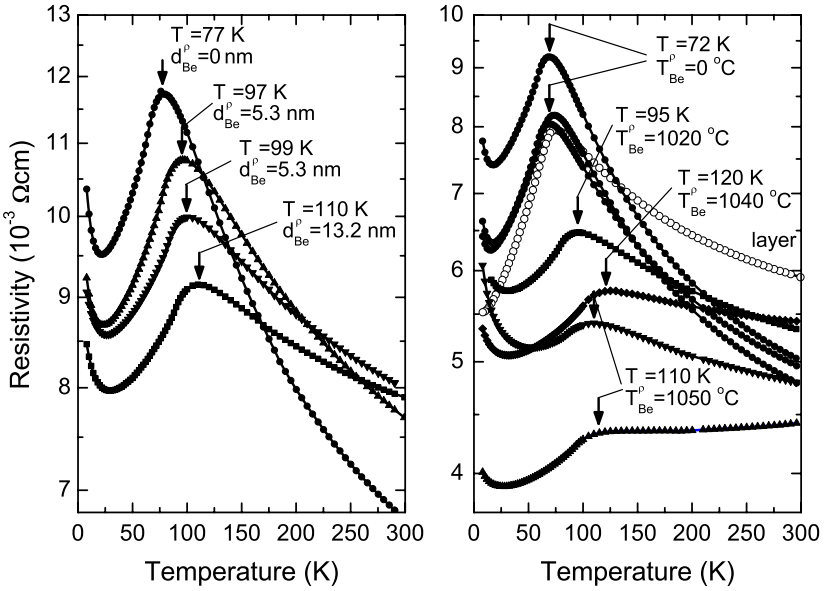

Figure 1. Temperature dependence of zero-field resistivities for $Ga_{1-x}Mn_xAs/Ga_{0.76}Al_{0.24}As$ heterojunctions remotely doped with Be acceptors. Left-hand panel: sample series with $x = 0.062$, $T_{Be} = 1040\,^{\circ}C$ and various d_{Be}. Right-hand panel: sample series with $x = 0.066$, $d_{Be} = 13.2$ nm, and various T_{Be}. In order to show reproducibility of the results, in the right-hand panel we also present data for three undoped heterojunctions. Also shown as the open symbols are data for a $Ga_{0.94}Mn_{0.66}As$ epilayer with no GaAlAs barrier. Sample parameters and peak resistivity values ($T_\rho \approx T_C$) are indicated in the figure.

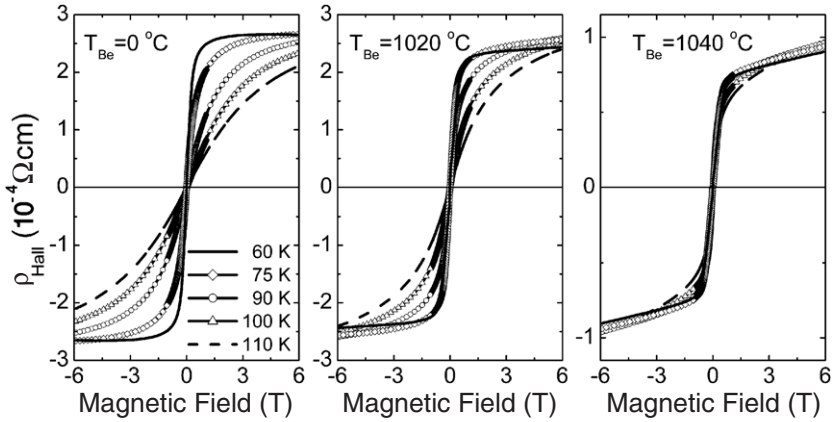

Figure 2. Field dependence of Hall resistivities ρ_{Hall} observed at various temperatures in three heterojunctions grown with different T_{Be}. The samples are the same as those discussed in the right-hand panel of figure 1.

The enhancement of T_C via modulation doping is further corroborated by direct SQUID magnetization measurements [12] (not shown) and by the studies of the anomalous Hall effect (AHE). The AHE results for three samples from the second series (grown with $T_{Be} = 0$, 1020 and 1040 °C, respectively) are given in figure 2. This figure shows the field dependence of the Hall resistivity ρ_{Hall} obtained at various temperatures, from 60 to 110 K.

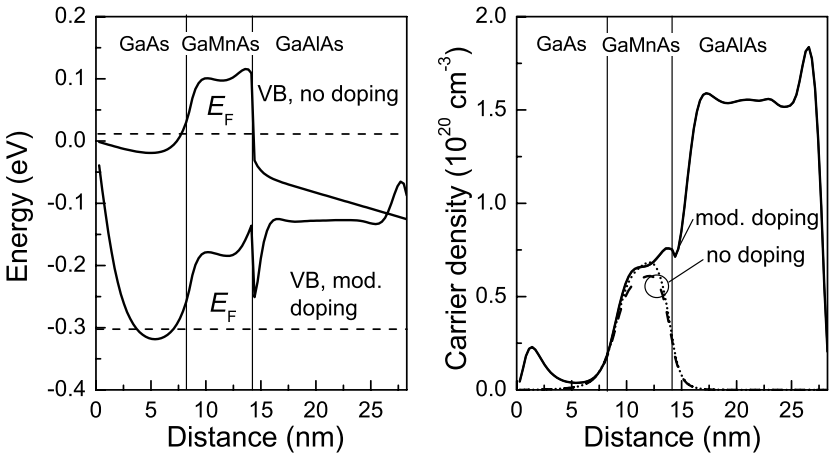

Figure 3. Results of theoretical calculations performed for a heterojunction with $x = 0.066$, carried out assuming (1) no modulation doping, and (2) that the concentration of uncompensated acceptors in the barrier is 3.1×10^{20} cm^{-3} (as determined from the Hall measurement performed on a thick $Ga_{0.76}Al_{0.24}As$:Be layer grown with $T_{Be} = 1050\,^{\circ}C$). The left-hand panel shows the valence band profiles (with Fermi levels marked by dashed lines). The valence band profiles and Fermi levels are offset for clarity for the two cases. The right-hand panel shows the spin-resolved hole densities (1) for just below the Curie temperature T_C (dashed and dotted curves for spin-up and spin-down, respectively) and (2) for just above T_C (solid curve). The spin-up and spin-down densities for the modulation-doped structure are seen to coincide above T_C. The increase of the hole concentration in $Ga_{0.934}Mn_{0.066}As$ layer close to $Ga_{0.76}Al_{0.24}As$ barrier is visible. The $Ga_{0.934}Mn_{0.066}As/Ga_{0.76}Al_{0.24}As$ valence band offset is taken to be 0.127 eV for this calculation.

One can clearly see that, while for undoped samples the anomalous Hall contribution to ρ_{Hall} decreases rapidly with increasing temperature (left-hand panel), this decrease becomes less pronounced with increasing Be doping level (i.e., with increasing T_{Be}). For the sample grown with $T_{Be} = 1040\,^{\circ}C$ all curves for various temperatures nearly coincide, indicating that T_C for this sample is around 110 K, in good agreement with $T_\rho = 120$ K. These data, as well as direct magnetization measurements [12], confirm the unambiguous increase of T_C with increasing modulation doping by Be.

Having established experimentally that the T_C of $Ga_{1-x}Mn_xAs$ can be enhanced by modulation doping, it is useful to determine whether a model for carrier-mediated ferromagnetism can reproduce such an increase. We have therefore simulated one of the heterojunctions from the second series ($x = 0.066$, $T_{Be} = 1050\,^{\circ}C$) using an eight-band effective bond-orbital-method calculation, that self-consistently includes magnetic interactions via mean field theory, as well as charge-transfer-induced electrostatic band bending via Poisson's equation [13]. The results of these simulations are presented in figure 3 for the following two cases: (1) for no modulation doping, and (2) for a concentration of uncompensated acceptors in the barrier of 3.1×10^{20} cm^{-3}. The left-hand panel shows the valence band profiles with the corresponding Fermi levels marked (offset for clarity for the two cases). The right-hand panel shows the spin-resolved hole densities (1) for just below the Curie temperature T_C (dashed and dotted curves for spin-up and spin-down polarizations, respectively); and (2) for just above T_C (solid curve). The spin-up and spin-down densities for the MD structure coincide above T_C. The peaks in the hole densities at the edges of the simulated regions (at distances of approximately 2 and 26 nm, respectively) are artefacts of the infinite-barrier/fixed electrostatic potential boundary conditions employed in the simulations.

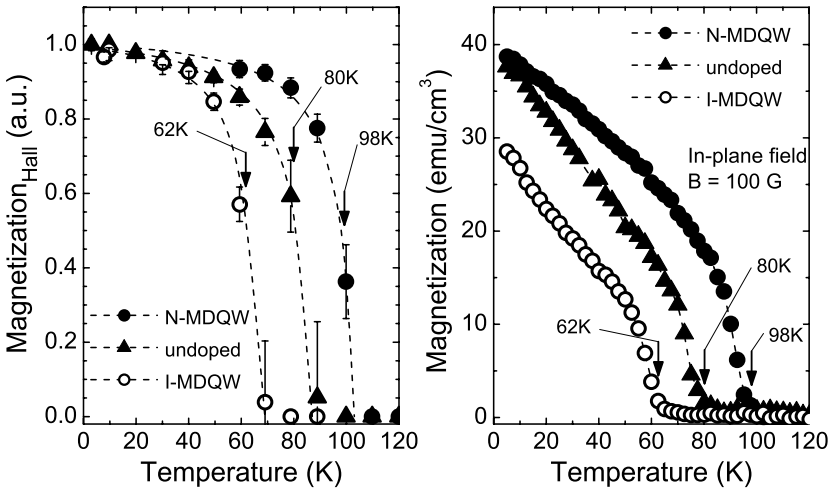

Figure 4. Left-hand panel: temperature dependence of normalized magnetization obtained from the Arrot plot analysis of the anomalous Hall effect data for three $Ga_{0.76}Al_{0.24}As/Ga_{0.938}Mn_{0.062}As/Ga_{0.76}Al_{0.24}As$ quantum well structures. Right-hand panel: temperature dependence of the remanent magnetization measured by SQUID with an in-plane magnetic field of 100 Gs for the same samples. Be acceptors were introduced either into the first barrier (that grown *before* the QW, I-MDQW), or into the second barrier (that grown *after* the QW, N-MDQW). The 'undoped' sample represents the heterostructure with no doping in either of the barriers. The curves are guides for the eye. The values of T_C determined from SQUID data are marked in both panels.

We have verified that the boundary conditions do not have a detectable impact on the calculated Curie temperatures.

On the other hand, the increase of the hole concentration in the $Ga_{0.934}Mn_{0.066}As$ layer close to the $Ga_{0.76}Al_{0.24}As$ barrier does lead to higher T_C and is clearly visible for the MD structure. In the calculations, the hole density in the undoped GaMnAs layer was chosen to fit the experimental $T_C = 70$ K observed in the absence of Be doping. For the Be-doped structure this calculation yields $T_C = 78$ and 85 K for two values of the $Ga_{0.934}Mn_{0.066}As/Ga_{0.76}Al_{0.24}As$ valence band offset: 0.127 eV (corresponding to a vanishing offset between GaAs and unmagnetized $Ga_{1-x}Mn_xAs$) and 0.25 eV, respectively. Note that even with the larger offset, the calculated Curie temperature is substantially smaller than the experimentally observed value of $T_C = 103$ K (figure 2). Thus, while our calculations do predict an increase of T_C associated with the enhanced hole concentration due to the modulation doping, the agreement is only qualitative. A likely explanation is that the substitutional Be incorporation into the $Ga_{1-y}Al_yAs$ barrier *is in fact enhanced* in the vicinity of the $Ga_{1-x}Mn_xAs$. The reduced Fermi energy in the barrier during its growth (because many of the holes are 'siphoned off' into the already-existing QW) should therefore induce an increase of the substitutional Be_{Ga} acceptor concentration, as compared to that measured in the doped calibration epilayer (and used in the calculations).

To demonstrate experimentally that the sequencing of layer growths plays a crucial role in the creation of Mn_I—and hence in the modification of T_C—we grew a series of low-temperature $Ga_{1-y}Al_yAs/Ga_{1-x}Mn_xAs/Ga_{1-y}Al_yAs$ QW structures in the following order: a structure with Be doping in the first barrier (so-called 'inverted modulation doped QW', I-MDQW); an undoped structure; and a structure with Be doping in the second barrier ('normal MDQW'—N-MDQW) [12]. The left-hand panel in figure 4 shows the temperature dependence of the

normalized magnetization obtained from the Arrot plot analysis of the anomalous Hall effect data (AHE) for this series. In the analysis the side-jump scattering mechanism was assumed to be dominant in the AHE. This method of accessing the modulation-doping-induced variation of the magnetic properties of heterostructures is in good agreement with the results obtained from resistivity [12] and SQUID magnetization measurements. The latter are presented in the right-hand panel of figure 4 in the form of temperature-dependent remanent magnetization. The values of T_C, taken to be the temperature at which the magnetization versus T drastically changes the slope before vanishing, are indicated with arrows in both panels. As compared to $T_C = 80$ K for the undoped sample, we find that—as in the previous series—T_C increases (to 98 K) for the N-MDQW sample doped *after* the QW was already grown; and it *decreases* (to 62 K) for the I-MDQW sample, doped *before* growing the QW, in agreement with our model of Fermi-energy-dependent creation of Mn_I.

It is important to emphasize that our experimental results—obtained on 'all-low-T-grown' MDQWs—are not at all inconsistent with the result of Nazmul *et al*, who observed T_C of 172 K in annealed Mn-delta-doped AlGaAs:Be/GaAs heterostructures, in which Be was introduced during the high-temperature part of the growth carried out before depositing the δ-Mn/GaAs layer at low-T [14, 15]. Our model of Fermi-energy-dependent creation of Mn interstitials is in fact consistent with the experimental results of Nazmul *et al* reported in [15] in two important respects. First, the increase of T_C from 0 K in undoped material to 70 K in selectively doped (unannealed) sample reported in [15] was observed in the situation where the Fermi energy E_F in δ-Mn doped GaAs—both with and without doping—was well below the maximum Fermi energy E_{Fmax}. The doping level of Nazmul *et al* was only 1.8×10^{18} cm^{-3} for a 30 nm-thick barrier. Assuming that all holes are transferred to the 3 nm-thick GaAs/δ-Mn region (see figure 2(e) in [15]), this gives the hole concentration of 1.8×10^{19} cm^{-3}—well below p_{max} corresponding to E_{Fmax} (in our studies we found p_{max} to be around 5×10^{20} cm^{-3} [8]). Additionally, the undoped structure of Nazmul *et al* was strongly compensated (thus having a very small E_F) and non-ferromagnetic due to the absence of a sufficient hole concentration, as claimed by the authors. Therefore in that system there was little or no Fermi-energy-induced creation of Mn interstitials in the sample where doping was done before the growth of the δ-Mn/GaAs layer. Furthermore, when E_F is well below E_{Fmax}, an increase of the hole concentration in the region where Mn_{Ga} is present should, according to our model, produce an increase of the Curie temperature, independent of the location of Be (whether Be is introduced before or after growing the QW). We have in fact already reported such an increase of T_C with increasing hole concentration in Be co-doped $Ga_{1-x}Mn_xAs$ layers having relatively small Mn concentration x—and hence a value of E_F below E_{Fmax} [11]. The data of Nazmul *et al* obtained on unannealed samples are therefore consistent not only with our model, but also with our earlier experimental data.

The second point of consistency of our model with the results [15] concerns the increase of T_C from 70 K in unannealed selectively doped sample to 172 K in the annealed sample reported by Nazmul *et al*. In their paper the authors did not specify the type of point defects whose concentration is reduced by their low-temperature annealing. Our model, on the other hand, provides such information. In our opinion the result of Nazmul *et al* indicates that Mn interstitials are an important source of electrical compensation not only in random alloy layers such as those which we studied, but also in Mn δ-doped samples. We note in passing that the enhancement of T_C via low-temperature annealing was one of the factors on which we have built our model (see [4]). In this respect the annealing result of Nazmul *et al* is not only consistent with our model, but in fact provides additional support for this picture.

Coming back to our results on the Fermi-energy dependent distribution of Mn on various III–V lattice positions, the enhanced incorporation of Mn into interstitial sites for structures

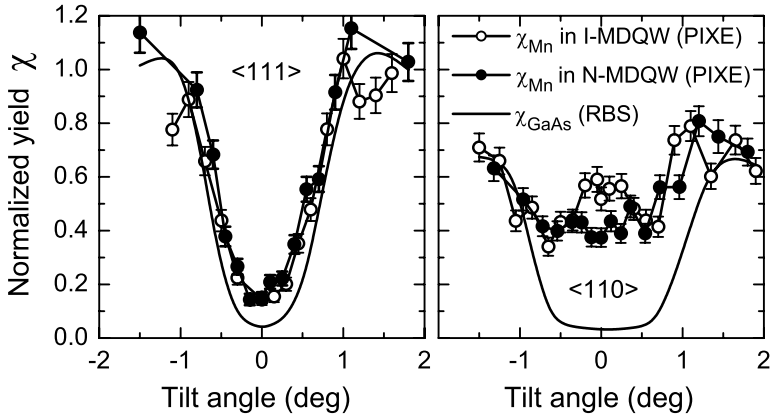

Figure 5. Normalized yields of the Mn (PIXE) and GaAs (RBS) signals for the $Ga_{0.938}Mn_{0.062}As$ QW layer in both I-MDQW and N-MDQW (the same as in figure 4) as a function of the incident tilt angles for angular scans about the ⟨110⟩ and ⟨111⟩ axes.

doped in the first barrier was unambiguously revealed by c-RBS/PIXE experiments [16]. Figure 5 shows the normalized yields of the Mn (PIXE) and GaAs (RBS) signals from the $Ga_{1-x}Mn_xAs$ QW for both I-MDQW and N-MDQW as a function of the incident beam angles about the ⟨110⟩ and ⟨111⟩ axes (angular scans). As seen in the left-hand panel of figure 5, the χ_{Mn} for both samples follows the χ_{GaAs} host very well for the ⟨111⟩ scans. The similarity of the χ_{Mn} and χ_{GaAs} curves observed for the ⟨111⟩ scan indicates that the Mn atoms not accounted by random clusters are shadowed by the Ga and As host atoms along this direction. However, this does not necessarily mean that they occupy substitutional sites in the lattice. The slightly higher χ_{Mn} in the ⟨111⟩ direction for both samples suggests that a small fraction (<10%) of Mn is in random positions not commensurate with the lattice. These random Mn atoms are most probably present as small clusters of Mn or MnAs [4].

This is made clear by the χ_{Mn} values for both samples in the ⟨110⟩ scans (shown in the right-hand panel of figure 5), which are distinctly higher than those in the ⟨111⟩ scans. This is similar to earlier observation on thicker $Ga_{1-x}Mn_xAs$ and $In_{1-x}Mn_xSb$ layers, where we interpreted this behaviour as an unambiguous signature for the presence of *interstitial* Mn atoms Mn_I [4, 8]. The difference in the respective Mn locations in the I-MDQW and N-MDQW is made clear in the Mn angular scans about the ⟨110⟩ axial channel shown in the right-hand panel of figure 5. The much higher χ_{Mn} in the ⟨110⟩ scan for the I-MDQW indicates that the concentration of Mn_I is higher in the $Ga_{1-x}Mn_xAs$ QW when the Be-doped barrier layer is grown prior to the deposition of the QW. Assuming the flux peaking in the ⟨110⟩ channel to be between 1.5 and 2.0 [4], we estimate the fractions of Mn_I to be ∼20% for I-MDQW and ∼11% for N-MDQW. We note that, within experimental error, the angular scans of the undoped heterostructure (not shown) are similar to the N-MDQW.

Results of RBS/PIXE studies presented in figure 5 provide direct experimental evidence that the manner of incorporation of Mn into $Ga_{1-x}Mn_xAs$ is *directly controlled by the Fermi energy during the growth itself*. These data also rule out the possibility that other effects—such as the competition between Mn and Be atoms to occupy the same substitutional sites—might be responsible for the increase in the number of Mn_I, since in modulation-doped structures Mn and Be atoms are spatially separated. Our studies of inverted- and normal-MDQW thus provide very strong support for the model of Fermi-level-induced limitation of T_C in $III_{1-x}Mn_xV$ [4, 7].

4. Conclusions

In summary, our results showing that T_C decreases rather than increases in both Be co-doped $III_{1-x}Mn_xV$ [8, 9] and in heterostructures remotely doped before the growth of ferromagnetic $Ga_{1-x}Mn_xAs$ (discussed in this paper) provide strong support for the model in which the incorporation of magnetically-active Mn acceptors in $III_{1-x}Mn_xV$ alloys, which requires the occupation of substitutional rather than interstitial sites, is governed by *electronic* considerations [4, 7]. This suggests that the strategy to further increase the Curie temperature of $III_{1-x}Mn_xV$ alloys should either be to use heavy n-type *counter-doping*—to allow increased incorporation of substitutional magnetically-active Mn for a constant $p = p_{max}$—or to use modulation doping in barriers grown *after* depositing the ferromagnetic QW structures—in order to raise p above the value p_{max} that is allowed during the deposition of the $III_{1-x}Mn_xV$ layer. The present experiments on modulation doping provide the 'proof of concept' for this second strategy.

Apart from providing an explanation for the limitation of T_C, our studies also have general implications for the understanding of defect formation during epitaxial growth generally. They clearly show that the formation of defects can be affected *by the growth sequence*, thus providing a handle for controlling the properties of epitaxial structures. For example, the present results provide direct support for the previously advanced explanation of differences in maximum mobility in the two-dimensional electron gas in inverted and normal GaAs/AlGaAs modulation-doped hererostructures (MDH) [17]. It has been argued in that context that the lower electron mobility observed in n-type inverted MDH results from a higher concentration of acceptor-like native defects. The formation of these defects is induced by the upward shift of the Fermi energy due to the transfer of electrons from the n-type modulation-doped AlGaAs barrier to the GaAs quantum well.

Acknowledgments

This work was supported by the DARPA SpinS Program under ONR Grant N00014-00-1-0951; by the Director, Office of Science, Office of Basic Energy Sciences, Division of Materials Sciences and Engineering of the US Department of Energy under Contract No. DE-AC03-76SF00098; and by NSF Grants DMR02-45227 and DMR02-10519.

References

[1] Ohno H 1998 *Science* **281** 951
[2] Dietl T 2002 *Semicond. Sci. Technol.* **17** 377
[3] Dietl T, Ohno H, Matsukura F, Cibert J and Ferrand D 2000 *Science* **287** 1019
[4] Yu K M, Walukiewicz W, Wojtowicz T, Kuryliszyn I, Liu X, Sasaki Y and Furdyna J K 2002 *Phys. Rev.* B **65** 201303-1(R)
[5] Wojtowicz T, Lim W L, Liu X, Sasaki Y, Bindley U, Dobrowolska M, Furdyna J K, Yu K M and Walukiewicz W 2003 *J. Supercond. Incorp. Novel Magn.* **16** 41
[6] Wojtowicz T, Cywinski G, Lim W L, Liu X, Dobrowolska M, Furdyna J K, Yu K M, Walukiewicz W, Kim G B, Cheon M, Chen X, Wang S M and Luo H 2003 *Appl. Phys. Lett.* **82** 4310
[7] Wojtowicz T 2003 *Bull. Am. Phys. Soc.* **48** 584
[8] Yu K M, Walukiewicz W, Wojtowicz T, Lim W L, Liu X, Sasaki Y, Dobrowolska M and Furdyna J K 2003 *Phys. Rev.* B **68** 041308-1(R)
[9] Wojtowicz T, Lim W L, Liu X, Cywinski G, Kutrowski M, Titova L V, Yee K, Dobrowolska M, Furdyna J K, Yu K M, Walukiewicz W, Kim G B, Cheon M, Chen X, Wang S M, Luo H, Vurgaftman I and Meyer J R 2004 *Physica* E **20** 325
[10] Blinowski J and Kacman P 2003 *Phys. Rev.* B **67** 121204(R)

[11] Lee S, Chung S J, Choi I S, Yuldashev Sh U, Im H, Kang T W, Lim W L, Sasaki Y, Liu X, Wojtowicz T and Furdyna J K 2003 *J. Appl. Phys.* **93** 8307
[12] Wojtowicz T, Lim W L, Liu X, Dobrowolska M, Furdyna J K, Yu K M, Walukiewicz W, Vurgaftman I and Meyer J R 2003 *Appl. Phys. Lett.* **83** 4220
[13] Vurgaftman I and Meyer J R 2001 *Phys. Rev.* B **64** 245207-1
[14] Nazmul A M, Sugahara S and Tanaka M 2002 *Appl. Phys. Lett.* **80** 3120
[15] Nazmul A M, Sugahara S and Tanaka M 2003 *Phys. Rev.* B **67** 241308-1(R)
[16] Yu K M, Walukiewicz W, Wojtowicz T, Lim W L, Liu X, Dobrowolska M and Furdyna J K 2004 unpublished
[17] Walukiewicz W and Haller E E 1991 *Appl. Phys. Lett.* **58** 1638